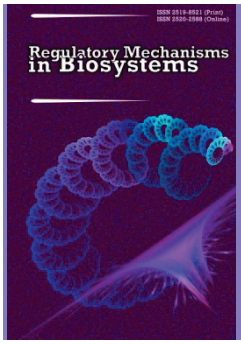

Regulatory Mechanisms in Biosystems

ISSN 2519-8521 (Print)
ISSN 2520-2588 (Online)
Regul. Mech. Biosyst.,
2024, 15(4), 688–695
doi: 10.15421/022499

Regulatory mechanisms in agroecosystems: A retrospective and forecast of spatial and temporal dynamics of precipitation as a factor of crop yield

Y. Nykytiuk*, O. Kravchenko**

*Polissia National University, Zhytomyr, Ukraine
**Kyiv Agrarian University of the National Academy of Agrarian Sciences, Kyiv, Ukraine

Article info

Received 26.08.2024
Received in revised form 03.10.2024
Accepted 12.10.2024

Polissia National University, Staryi Boulevard, 7, Zhytomyr, 10008, Ukraine. Tel.: +38-097-770-65-02. E-mail: r.alimovih@gmail.com

Kyiv Agrarian University of the National Academy of Agrarian Sciences, Vasylkivska st., 37, Kyiv, 03022, Ukraine. Tel.: +38-067-448-38-48.

Nykytiuk, Y., & Kravchenko, O. (2024). Regulatory mechanisms in agroecosystems: A retrospective and forecast of spatial and temporal dynamics of precipitation as a factor of crop yield. Regulatory Mechanisms in Biosystems, 15(4), 688–695. doi:10.15421/022499

The research tested the hypothesis that the climate of the studied area has the property of spatial and temporal regularity, and that this regularity is hierarchically organized, which makes it possible to predict the state of the climate in the coming decades. The practical aspect of the information obtained is the assessment of possible prospects for changes in the yields of the most common crops in the region. The spatial variability of precipitation between the years 1960 and 2023, soil properties and landscape cover structure were investigated within 10 administrative regions of northern and northwestern Ukraine. This region covers the Polissia and Forest-Steppe geographical zones. The MEM spatial variables were able to explain 95.1% of the variability in precipitation. ANOVA revealed that 8 canonical axes were statistically significant. The contribution of the spatial MEM variables to the explanation of the canonical axes is different, which allows us to identify the hierarchical structure of variability of the main spatial precipitation patterns in the region. The RDA1 and RDA2 axes represent the large-scale component of precipitation variability. RDA1 indicates the differentiation of precipitation patterns in the meridional direction with the allocation of the eastern and western sectors of the region. The canonical axes denoting the main spatial patterns of precipitation variability correlated with soil properties and land cover types. RDA1 did not correlate with soil properties, but had a positive correlation with the proportion of broadleaf forests and mosaic of herbaceous cover and shrubs in the landscape cover. This axis had a negative correlation with the proportion of agricultural land. RDA2 was positively correlated with soil organic matter and sand content, but negatively correlated with clay and silt content. This axis increased with an increase in the proportion of broadleaf, coniferous or mixed forests or a mosaic of herbaceous vegetation and shrubs in the landscape cover structure. RDA2 decreased with an increase in the proportion of agricultural crops or sparse vegetation cover. RDA3 was independent of soil organic matter content, but positively correlated with clay and silt content and negatively correlated with sand content. This axis was positively correlated with the proportion of agricultural area, the mosaic of herbaceous vegetation and shrubs, and negatively correlated with the proportion of coniferous or mixed forests. RDA4 was positively correlated with soil organic matter content and negatively correlated with soil silt content. This axis increased with increasing proportions of rainfed crops and sparse vegetation cover, but decreased with increasing proportions of herbaceous cover, coniferous and mixed forests. RDA5 was positively correlated with organic matter and silt content, but negatively correlated with sand content. This axis increased with increasing proportions of mosaic with crops, but decreased with increasing proportions of coniferous and mixed forests. RDA6 was positively correlated with silt content but negatively correlated with sand content. This axis increased with increasing proportions of agricultural crops, but decreased with increasing proportions of broadleaf or mixed forests. RDA7 was positively correlated with silt and clay content, but negatively correlated with organic matter and sand content. This axis was positively correlated with the proportion of agricultural land and negatively correlated with the proportion of broadleaf, coniferous and mixed forests. RDA8 was positively correlated with the silt content of the soil. This axis was positively correlated with the proportion of agricultural land and negatively correlated with the proportion of coniferous and mixed forests. The temporal modelling of precipitation dynamics over more than 60 years can be carried out using eight AEM predictors, which represent temporal patterns of different frequencies and variable amplitudes over time. If we assume that the established oscillatory dynamics will continue in the coming decades, then these AEM predictors can be extended for the time of interest and a regression model can be used to obtain a forecast of precipitation dynamics in the near future. The forecast indicates a downward trend in precipitation, mainly in areas with the most developed agriculture.

Keywords: climate change; spatial pattern; temporal dynamic; landscape; soil cover.

Introduction

Precipitation is a critical factor in climate and hydrometeorology, and a major driver of hydrological processes, terrestrial ecosystem structure, and function (Emmanuel et al., 2012), which determine the conditions of agricultural production (Hernández-Rodríguez et al., 2023). The precipitation patterns are highly variable, with significant differences in frequency, duration, intensity and overall trend over time. These patterns directly influence the rhythm of water use by humans and ecosystems (Sang et al., 2020). It is indisputable that changes in precipitation have a significant impact on the hydrological cycle and human life. They can also lead to floods, droughts, biodiversity loss, reduced agricultural productivity and soil erosion (Sayemuzzaman & Jha, 2014). There is no doubt that an increase in extreme precipitation events will lead to an increased risk of flooding, especially given the rapid urbanisation that is currently taking place (Nguyen et al., 2019). It is a fact that high temperatures have a negative impact on yields. This is due to heat stress and soil moisture deficits. Similarly, low precipitation leads to stomatal closure, reduced carbon uptake and lower yields (Butler & Huybers, 2013). Modern statistical procedures provide unquestionably powerful tools for predicting crop yields under global climate change, even if the model is based on only climate variables such as temperature and precipitation (Leng & Hall, 2020).

Precipitation forecasting is the process of using a range of models and data sources to accurately predict the amount and timing of precipitation, such as rain or snow, in a given area. Further forecasts are based on historical data on precipitation dynamics (Claußnitzer & Névir, 2009). Mathematical and statistical methods allow the accurate prediction of future precipitation trends. They enable the identification of patterns, changes and relationships in the data (Benziane, 2024). The most common statistical methods are trend analysis, frequency or spatial analysis, regression models and time series models. Identifying periodic rainfall fluctuations is the most important aspect of rainfall modelling and forecasting (Sang et al., 2020). The seasonality of the precipitation regime and the amount of precipitation allowed us to identify clear spatial structures. These structures were then used to identify the dominant factors influencing the spatial variability of precipitation (Sariş et al., 2010). Spatial variations in precipitation at scales of 10–160 km undoubtedly influence the vegetation structure and migratory fauna of the steppe. This has significant implications for livestock producers and future climate change assessments (Augustine, 2010).

Precipitation is a distinct field of study within climatology and meteorology. However, precipitation forms an aspect of climate that affects biological systems and is therefore a climatope (Kyyak et al., 2023). A climatope is a specific climatic regime that allows for the formation of a spatially regular fragment of landscape cover. Together with the edaphotope, it forms an ecotope. It must be emphasised that, just as an edaphic environment is not equivalent to soil, a climatological environment is not equivalent to climate. An edaphotope is the way in which living organisms perceive soil. Similarly, the climatope is an aspect of the ways in which living organisms perceive climate. The system is becoming more complex. It is no longer sufficient to consider only the climatic component; the biotic component must also be taken into account. Conversely, a specific list of purely climatic issues recedes into the background. For example, this approach does not require an explanation of the mechanisms and processes of the dynamics of climatic phenomena. Climate can be considered purely phenomenologically or formally. This approach can be interpreted as ecological within the framework of ecological climatology. Our study aimed to test the hypothesis that the climate of the area under investigation exhibits spatial and temporal regularity, which is hierarchically ordered. This allows us to predict the state of the climate in the coming decades. The practical aspect of the information obtained is to assess the possible prospects for changes in the yield of the most common crops in the region.

Materials and methods

We investigated the spatial variability of precipitation between the years 1960 and 2023, soil properties and landscape cover structure within 10 administrative regions of northern and northwestern Ukraine. This region encompasses both the Polissia and Forest-Steppe geographical zones. The environmental characteristics were averaged within the administrative regions before Ukraine's 2015–2022 reform of its administrative and territorial structure. This is because the area of "traditional" rayons (administrative districts) is smaller and more ecologically homogeneous than that of the new administrative units. Furthermore, data on crop yields have been collected for a long time within the "old" administrative districts, which is essential for understanding the relationship between productive potential and soil and landscape conditions. The spatial variability of the region's soil cover was obtained from the Harmonized World Soil Database (Version 2.0). Information on soil properties was obtained from the SoilGRIDS database (www.isric. org/explore/soilgrids) using the geodata package. Information on landscape cover types was obtained from the GlobCover Land Cover Maps database (http://due.esrin.esa.int/page_globcover.php). The historical data on the spatial variability of precipitation were obtained from the WorldClim website (www.worldclim.org).

Assessing meteorological dynamics is a complex task, given the variability of hydroclimatic conditions. A variety of statistical analyses are used to describe hindcast data and to forecast precipitation. The following five approaches form the basis of such methods (Benziane, 2024). 1. Descriptive statistics are used to describe the characteristics of a particular data set. This method involves summarising and describing the properties of a given data set, including measures such as the mean, median, mode, standard deviation and range (Bougara et al., 2020). Descriptive statistics are the ideal tool for examining the distribution and variability of rainfall data (Ellouze et al., 2009). 2. Correlation analysis allows us to study the relationship between two variables (Harbar et al., 2024). This enables us to determine the strength and direction of the relationship between, for example, precipitation and temperature (Kassaye et al., 2022). Correlation analysis is the most effective method for identifying patterns and associations in rainfall data (Seo et al., 2019). 3. Regression analysis is an invaluable tool for investigating the interdependencies between multiple climate variables (Steele et al., 2005). This approach involves constructing a model to establish the relationship between a dependent variable, such as precipitation, and one or more independent variables, including temperature, humidity, topography, landscape, and vegetation structure (Mykhailyuk et al., 2023). Regression analysis is the most effective method for predicting rainfall based on other meteorological variables (Latif et al., 2023). 4. Time series analysis is a statistical technique that identifies trends, patterns and seasonal variations in a sequence of observations over time. These observations can be daily or monthly rainfall data, for example (Pham et al., 2020). This method is an effective way to identify trends, patterns and seasonal variations in data. It involves examining a sequence of observations over time, such as daily or monthly rainfall data (Papalaskaris et al., 2016). Time series analysis is an effective tool for predicting future precipitation patterns (Hendri & Fadhlia, 2024). 5. Spatial analysis allows us to confidently examine precipitation data over a geographic region, such as a country or continent, to identify clear patterns and variations in the amount and distribution of precipitation (Charles et al., 2024). By using spatial analysis, it is possible to determine which areas are most vulnerable to drought or flooding (Roldán-Valcarce et al., 2023).

The response of crops to environmental factors or the dynamics of seasonal signatures can be modelled using several nonlinear functions $f\theta rs$. The asymmetric Gaussian function (AG) has a mathematical form that is ecologically meaningful and can be interpreted in this way (Lewis-Beck et al., 2020). The AG function is the best way to describe the data and is superior to other curves (Jonsson & Eklundh, 2002), such as the double logistic, for comparing with empirical data (Hird & McDermid, 2009). The full functional form for the AG curve is shown in the equation. It is clear that the function argument, d (precipitation), determines which half of the AG curve is activated. If d is less than (greater than) δ, then the first (second) Gaussian curve determines the function form for the value of the function argument d (Wallis, 2014):

$$f_{\theta}^{AG}(d) = \begin{cases} \beta + (\mu - \beta) exp\left[-\frac{(d-\delta)^2}{2\sigma_1^2}\right] & d \le \delta \\ \beta + (\mu - \beta) exp\left[-\frac{(d-\delta)^2}{2\sigma_2^2}\right] & d > \delta \end{cases},$$

where δ is the maximum value of y, β is the parameter controlling the lower values, μ is the break-point separating the first and second half-bell curve, σ_1 is the scale for the first half of the bell-shaped curve which is the rate of culture yield increase due to precipitation increase, σ_2 is the scale for the second half of the bell-shaped curve which is the rate of culture yield decrease due to precipitation increase. AG parameters with an ecological meaning are calculated as $L = (\sigma_1 + \sigma_2)\sqrt{2\ln_2}$, and this is the tolerance of the crop to the environmental factor. In terms of the AG function, this is interpreted as the distance between the left and right inflection points of the AG curve. The function was fitted in the nlraa package. Descriptive statistics, cluster and discriminant analysis of streets were calculated in StatSoft 12.0.

The spatial configuration of the centroids of administrative districts was accurately described using distance-based maps of Moran's eigenvectors (dbMEM). This method is based on the calculation of the main coordinates of the geographical neighbours matrix (Dray et al., 2006). The MEM analysis method is the best way to identify spatial patterns of environmental variability (Blanchet et al., 2008). Time patterns were modelled using AEM variables (Baho et al., 2015).

Results

Spatial variation in precipitation. MEM spatial variables were able to explain 95.1% of precipitation variability ($F = 49.1$, $P < 0.001$). ANOVA

revealed that 8 canonical axes are statistically significant (Fig. 1). The contribution of the spatial MEM variables to the explanation of the canonical axes was different, which allowed us to identify a hierarchical structure of variability of the main spatial precipitation patterns in the region (Fig. 2). The RDA1 and RDA2 axes denote the large-scale component of precipitation variability. RDA1 indicated the differentiation of precipitation patterns in the meridional direction with the allocation of the eastern and western sectors of the region. RDA1 showed autocorrelation in time with a lag of 5 years ($r = –0.18$, $P = 0.05$). RDA2 differentiates the region into the central and southern sectors on the one hand and other parts of the region on the other. RDA2 exhibits autocorrelation in time with a lag of 3 years ($r = –0.22$, $P = 0.03$). The broad-, medium-, and fine-scale spatial components are represented in the variation of the RDA3 axis. This axis differentiates precipitation dynamics in the northern and central parts on the one hand and the southeastern and southwestern parts on the other. RDA3 shows autocorrelation in time with a lag of 2 years ($r = –0.13$, $P = 0.05$). The broad-, medium-, and fine-scale spatial components are represented in the variation of the RDA4 axis, but the fine-scale component prevails. This axis differentiates precipitation dynamics in the northwestern and southeastern parts on the one hand and in a diagonal segment covering the northeastern, central, and southwestern parts on the other. RDA4 shows autocorrelation in time with a lag of 1 year ($r = +0.13$, $P = 0.05$). The variation of the RDA5 axis is mainly represented by a broad-scale spatial component. This axis differentiates precipitation dynamics in the eastern and southwestern parts on the one hand, and in the western part and diagonal from northwest to southeast on the other hand. RDA5 demonstrates autocorrelation in time with a lag of 1 year ($r = –0.37$, $P < 0.01$) and a lag of 2 years ($r = +0.35$, $P < 0.01$). The variation of the RDA6 axis represents the broad- and medium-scale spatial components. This axis differentiates precipitation dynamics from the axis of symmetry along the longitudinal direction. RDA6 demonstrates autocorrelation in time with a lag of 9 years ($r = –0.28$, $P < 0.01$) and a lag of 12 years ($r = +0.22$, $P = 0.02$). The variation of the RDA7 axis includes broad-, medium-, and fine-scale spatial components, but the broad-scale component predominates. This axis represents a complex island-like pattern of precipitation variability. RDA7 shows autocorrelation in time with a lag of 3 years ($r = 0.24$, $P = 0.02$) and a lag of 13 years ($r = –0.25$, $P = 0.01$). The variation of the RDA8 axis includes broad-, medium-, and fine-scale spatial components, but the medium-scale component predominates. This axis represents a complex island-like pattern of precipitation variability. RDA8 shows autocorrelation in time with a lag of 9 years ($r = –0.23$, $P = 0.01$).

The role of environmental determinants in the generation of spatial patterns of precipitation. The canonical axes representing the main spatial patterns of precipitation variability correlated with soil properties and land cover types (Table 1). RDA1 did not correlate with soil properties, but had a positive correlation with the proportion of broadleaf forests and mosaics of herbaceous and shrubs in the landscape cover. This axis had a negative correlation with the proportion of agricultural land. RDA2 was positively correlated with soil organic matter content and sand content, but negatively correlated with clay and silt content.

This axis increased with an increase in the proportion of broadleaf, coniferous or mixed forests or a mosaic of herbaceous vegetation and shrubs in the landscape cover structure. RDA2 decreased with an increase in the proportion of agricultural crops or sparse vegetation cover. RDA3 was independent of soil organic matter content, but positively correlated with clay and silt content in the soil and negatively correlated with sand content in the soil. This axis was positively correlated with the proportion of agricultural land, the mosaic of herbaceous vegetation and shrubs, and negatively correlated with the proportion of coniferous or mixed forests. RDA4 was positively correlated with soil organic matter content and negatively correlated with soil silt content. This axis increased with an increase in the proportion of rainfed crops and sparse vegetation cover, but decreased with an increase in the proportion of herbaceous cover, coniferous and mixed forests. RDA5 was positively correlated with organic matter and silt content, but negatively correlated with sand content. This axis increased with increasing proportions of mosaic with crops, but decreased with increasing proportions of coniferous and mixed forests. RDA6 was positively correlated with silt content but negatively correlated with sand content. This axis increased with increasing proportions of agricultural crops, but decreased with increasing proportions of broadleaf or mixed forests. RDA7 was positively correlated with silt and clay content, but negatively correlated with organic matter and sand content. This axis was positively correlated with the proportion of agricultural land and negatively correlated with the proportion of broadleaf, coniferous, and mixed forests. RDA8 was positively correlated with the silt content of the soil. This axis was positively correlated with the proportion of agricultural land and negatively correlated with the proportion of coniferous and mixed forests.

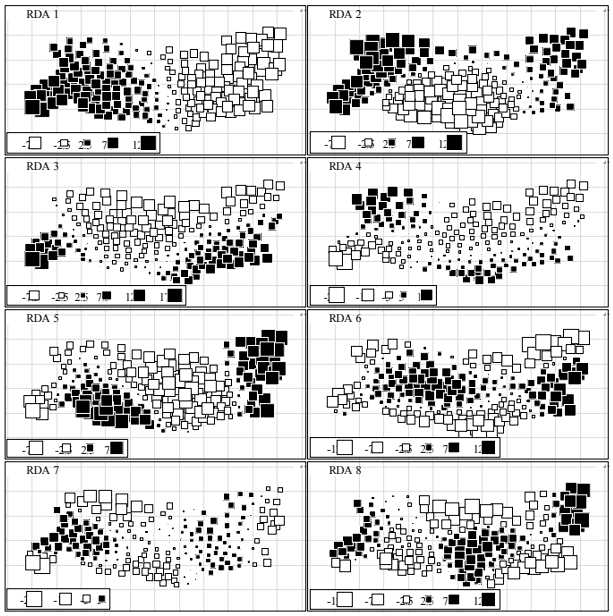

Fig. 1. Spatial variability of the canonical axes selected after conditional redundancy analysis with spatial MEM variables as predictors: RDA1 explains 49.9% of precipitation variation ($F = 161.3$, $P < 0.001$), RDA2 explains 23.1% of precipitation variation ($F = 62.5$, $P < 0.001$), RDA3 explains 14.1% of precipitation variation ($F = 34.5$, $P < 0.001$), RDA4 explains 4.8% of precipitation variation ($F = 11.5$, $P < 0.001$), RDA5 explains 4.0% of the variation in precipitation ($F = 9.6$, $P < 0.001$), RDA6 explains 1.9% of the variation in precipitation ($F = 5.0$, $P < 0.001$), RDA7 explains 0.9% of the variation in precipitation ($F = 2.9$, $P = 0.023$), RDA8 explains 0.5% of the variation in precipitation ($F = 2.1$, $P = 0.048$)

Temporal patterns of precipitation variability for the forecast. The temporal AEM predictors 9, 25, 31, 32, 36, 43, 46, and 61 were able to statistically significantly predict temporal patterns of precipitation variability within the study area (Fig. 3). These predictors explained 35.2% of the variability of the total precipitation matrix over time ($F = 5.3$, $P < 0.001$). The AEM predictors were able to explain 35 to 94% of the variability in precipitation within a given administrative region. The highest explanatory power of the AEM predictors was found for the southern and southeastern regions, and the lowest for the western and northeastern regions. The AEM predictors represent regular oscillatory processes, so they can easily be extended into the future, which can be used to make a forecast of precipitation dynamics in the near future. The forecast for administrative regions was made for the period up to 2060 (Fig. 4). Spatial slices of precipitation variability for demonstration purposes were made for 2040 and 2060 (Fig. 5). In 2040, the zone of minimum precipitation will be located in the central and southeastern parts of the region. In 2060, the total precipitation level will be lower, and the zone of localized minimum precipitation will be spread throughout the east and center of the region.

The role of precipitation in crop yield variability. Precipitation generates an environmental gradient, and the response of crops to it follows an asymmetric Gaussian curve. For all crops, except sugar beet, the sigma 1 parameter was smaller than the sigma 2 parameter (Table 2), indicating that crops are more sensitive to drought than to excessive precipitation. Estimates of the optimal precipitation level for crops are most often close to the lower value in the range according to FAO estimates. The crops

differ in their tolerance to rainfall. The most tolerant are rapeseed, wheat and rye, while the least tolerant are soybeans and sugar beets.

Discussion

The regions of Polissia and the Forest-Steppe represent significant areas of Ukraine with considerable potential for the advancement of agricultural and forestry activities. It is essential that any active economic utilisation of the territory is undertaken in a manner that ensures the continued sustainability of the ecological systems in question, whilst simultaneously supporting the fulfilment of the ecosystem functions. The effects of climate change and the impact of these processes, in addition to the intensity of soil erosion, have the potential to significantly affect the sustainability of agricultural production and forestry. Ecological systems are widely acknowledged as one of the most intricate and challenging areas of study, given their composition of numerous diverse components, nonlinear interactions between them, extensive structural and functional diversity at large scales, and spatial heterogeneity. The advent of sophisticated spatio-temporal ecological datasets is becoming increasingly prevalent in ecology, driven by the growing utilisation of large-scale simulation models and automated data collection tools (Steele et al., 2005). The spatial variation of precipitation within the studied region is a largely spatially structured process, as evidenced by regression analysis with MEM variables as predictors. The spatial structure at different spatial scales can be flexibly modelled based on a set of uncorrelated component models, such as Moran's eigenvector (MEM) maps, which are derived from the spatial relationships between sample points, as defined in the spatial weight matrix (Wagner, 2013). The descriptive statistics of continuous monthly and annual precipitation data afford the opportunity to monitor the spatial and temporal variability of precipitation characteristics (Ellouze et al., 2009). Principal component analysis and multiple regression methods enable the characterisation of precipitation distribution in space and time, as well as the identification of the dominant variables associated with its variability. The correlation analysis demonstrated that changes in land use/cover types exert a predominant influence on precipitation dynamics. Furthermore, precipitation is also contingent on the variation in elevation (Kassaye et al., 2022). These findings are consistent with those of other studies. For instance, it has been demonstrated that precipitation variability is contingent upon seasonal conditions, with longitude exhibiting the greatest explanatory power. The primary determinant of spatial patterns is topography (Ellouze et al., 2009). Additionally, evidence suggests that maximum and minimum temperature fluctuations are most influenced by elevation. No significant correlation was identified between catchment size and precipitation variability (Kassaye et al., 2022).

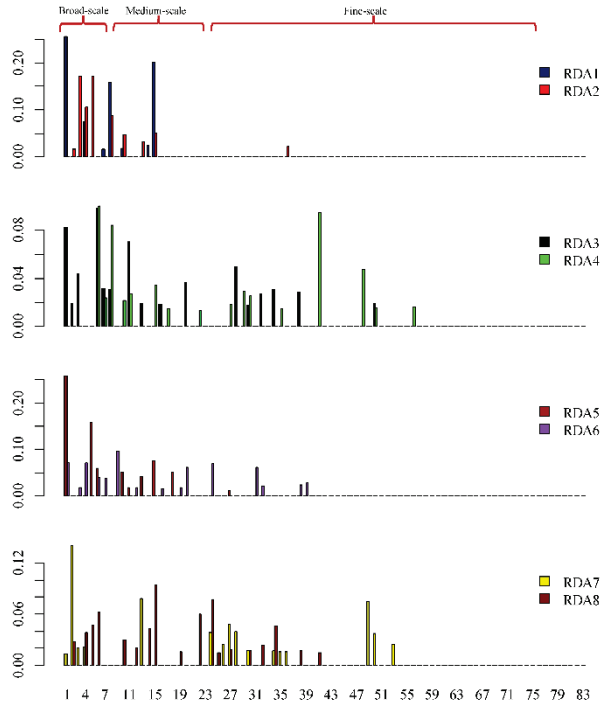

Fig. 2. Scalogram of the variability of the canonical axes selected after conditional redundancy analysis with spatial MEM variables as predictors: the abscissa axis is the order of spatial MEM variables (1 is the most broadly scaled variable, 83 is the most finely scaled variable); the MEM variables were conditionally grouped into broad-scale (1–10), medium-scale (11–20), and detailed-scale (21–83)

The peculiarity of our results is that we have proved the hierarchical nature of the spatial structure of precipitation variability. The spatial patterns of variability were divided into broad-, medium-, and fine-scale patterns. Usually, broad-scale spatial patterns are induced by abiotic factors, while detailed-scale patterns are the result of the action of factors of biotic origin (Kraan et al., 2015).

Table 1

Correlation between the redundancies identified after conditional analysis with spatial MEM variables as predictors and ecological properties of the territories (correlation coefficients are statistically significant for $P < 0.05$)

Variables	RDA 1	RDA 2	RDA 3	RDA 4	RDA 5	RDA 6	RDA 7	RDA 8
Soil properties:								
Organic matter	–	0.40	–	0.33	0.24	–	–0.38	–
Clay	–	–0.66	0.61	–	–	–	0.18	–
Sand	–	0.64	–0.51	–	–0.16	–0.22	–0.30	–
Silt	–	–0.54	0.37	–0.21	0.23	0.32	0.35	0.16
Types of landscape cover (GlobCover):								
Rainfed croplands	–	–0.62	0.33	0.26	–	0.16	0.27	0.22
Mosaic Croplands (50–70%) / Vegetation (grassland/shrubland/forest) (20–50%)	–0.38	–0.34	–	–	0.28	0.18	0.38	0.19
Mosaic vegetation (grassland/ shrubland/ forest) (50–70%) / cropland (20–50%)	–	–0.22	0.60	–0.29	0.18	–	–	–
Closed (>40%) broadleaved deciduous forest (>5 m)	0.36	0.55	–	–	–	–0.14	–0.22	–
Closed (>40%) needle-leaved evergreen forest (>5 m)	–	0.25	–0.37	–0.22	–0.25	–	–0.23	–0.36
Open (15–40%) needle-leaved deciduous or evergreen forest (>5 m)	–0.16	0.42	–0.38	–0.20	–	–0.34	–	–
Closed to open (>15%) mixed broadleaved and needle-leaved forest (>5 m)	–	0.46	–0.46	–	–0.26	–0.14	–0.36	–0.26
Mosaic grassland (50–70%) / forest or shrubland (20–50%)	0.52	0.26	0.34	–0.27	–	–	–	–
Closed to open (>15%) herbaceous vegetation (grassland, savannas or lichens/mosses)	0.32	0.22	0.29	–0.22	–	–	–	–
Sparse (<15%) vegetation	–0.16	–0.50	0.27	0.22	–	–0.28	–	–
Closed to open (>15%) grassland or woody vegetation on regularly flooded or waterlogged soil – Fresh, brackish or saline water	–	–	–0.21	–	–	–	–0.23	–0.22
Artificial surfaces and associated areas (Urban areas >50%)	–	–	–	–	–	–	–	–

The broad-scale patterns of precipitation may be explained by the geographical factors such as longitude and latitude zonation. The medium-scale patterns of variability are the result of the influence of geological and morphological factors on precipitation dynamics, which are also reflected in the structure of the soil cover, which is why soil characteristics are reliable predictors of the corresponding climate patterns. Fine-scale patterns can be explained by the influence of landscape cover diversity. Thus, the spatial variability of total precipitation in the study area is the result of a

complex of factors that manifest the patterns of geographic and altitudinal zonation, as well as geographic sectoralization (meridional zonation).

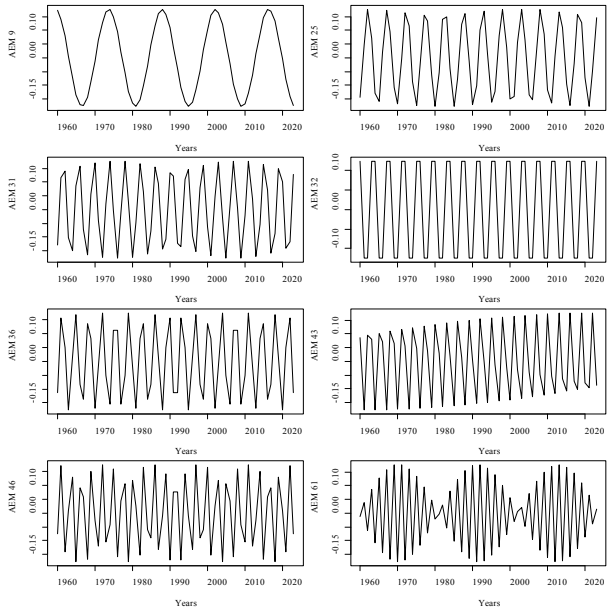

Fig. 3. AEM-predictors 9, 25, 31, 32, 36, 43, 46, and 61 were able to statistically significantly predict temporal patterns of precipitation variability within the study area

The main spatial patterns of precipitation that can explain a significant portion of the variability of this indicator are subject to zonation: latitudinal and meridional. Meridional zonation is the result of the continentality factor and is the most important factor in the differentiation of precipitation in space. The study area is divided into two large zones: eastern and western, which is clearly reflected in the spatial variability of RDA1. The zonal aspect of variability, which is sensitive to the differences between mixed forest and forest-steppe zones, is denoted by RDA2 and RDA3, even though these axes formally carry independent information. Obviously, the zonal nature of precipitation variability is also subject to the corrective influence of the spatial distribution of soil properties and land cover types. Both of these axes are sensitive to the proportion of the area covered by agricultural land. It can be assumed that certain variations in the zonal pattern were induced by anthropogenic factors. Surface evaporation is known to have a significant impact on precipitation (Wei & Dirmeyer, 2019). Agricultural land significantly changes the intensity of moisture evaporation from the Earth's surface (Blyth et al., 2006), which can explain the impact of land on precipitation (Kunakh et al., 2020). It is most likely that the homogeneous zonal pattern of precipitation variation has undergone a transformation due to the heterogeneous agricultural development within the territory (Kunakh et al., 2023). This anthropogenic factor is the result of both natural features, namely the distribution of soil fertility and its suitability for growing the respective crops, and factors such as logistical accessibility, population density, and demographic or historical reasons.

It is important to highlight that the proportion of agricultural land has an impact on the formation of all precipitation spatial patterns modelled by RDA1-RDA8. It is evident that agricultural areas exhibit notable differences in characteristics when compared to the natural vegetation cover, which is predominantly comprised of forest types, including coniferous, broadleaf, and mixed forests. This contrast affects the dynamics of the water cycle and the energy exchange of the Earth's surface, which in turn affects precipitation dynamics (Lobachevska & Karpinets, 2024). The spatial distribution of natural ecosystems is characterised by a complex hierarchical structure (Wu & David, 2002). Each component of the microclimatic environment exhibits distinctive spatial and temporal responses to alterations in structural elements. The diverse array of natural vegetation types exerts varying influences on the progression of microclimatic processes within the atmosphere (Mughal et al., 2021). In forest landscapes, the fundamental units of landscape structure emerge from disturbances and alterations to the physical and geomorphological environment, exhibiting a close correlation with the attributes of vegetation and soil cover (Forman, 1995). The microclimate within each landscape structure unit is distinct (Chen et al., 1996). The biodiversity within landscape structural units is directly determined by microclimatic differences (Forman, 1995). The daytime shortwave radiation, temperature, and wind speed are typically higher in anthropogenically transformed landscape units than in undisturbed areas. Disturbances exhibit greater spatial variation and temporal variability of energy components, which significantly affects the evaporation of the Earth's surface (Chen et al., 1993). The water balance of the landscape and the overall level of evaporation are significantly affected by natural and artificial forests (Qingming et al., 2022), which can explain the spatially hierarchical structure of precipitation in the study area.

The relationship between the productivity of soybean, sunflower, and winter rye cultivation and landscape diversity is demonstrated for the Polissia and Forest-Steppe regions (Kukol et al., 2024). The strongest statistical relationship between yields and landscape diversity indicators was identified for soybean yields, while sunflower yields exhibited the least dependence on landscape diversity. The majority of the relationships are nonlinear, indicating that there is an optimal level of landscape diversity that can be achieved to attain the highest possible crop yields (Zymaroieva et al., 2019; Zymaroieva et al., 2021). The climatic and soil conditions prevailing in a given area exert a considerable influence on the yield of sunflowers. The variation in sunflower yield trend parameters in Polissia and the Forest-Steppe is explained by edaphic and climatic factors to a significant extent, with the proportion of the variation explained ranging from 34% to 58%. Among the edaphic factors that determine the variability of sunflower yields, soil texture and soil organic carbon content are of particular significance.

The primary climatic determinants of sunflower yield are the continental climate and the degree of temperature variability during the growing season (Zymaroieva et al., 2021). The principal component analysis of grain and legume yield variability identified seven principal components, which collectively account for 66.8% of the total yield variability. Crop yield fluctuations over a period of ten years or more may be attributed to climatic factors. Among the various agro-environmental factors, climate change has been identified as the primary driver of crop yield fluctuations (Zymaroieva & Zhukov, 2020). A common feature of temporal changes in soybean yields for the administrative regions of Polissia and the Forest-Steppe is the presence of a trend that has an agroeconomic origin. The maximum rate of decline and the maximum rate of increase in yield are proposed as markers of the agroecosystem's resistance to agroeconomic factors. The southern and eastern regions of the study area exhibit the greatest sensitivity to agrotechnological and agroeconomic factors, while the northern and western regions demonstrate the lowest sensitivity (Zymaroieva et al., 2020). The yields of rapeseed in Polissia and the Forest-Steppe during the period between 1991 and 2017 were influenced by a number of agroeconomic and agrotechnological factors, which can be identified as the determinants of the general trend observed.

The mapping of maximum rates of yield decline and growth enables the identification of areas where yields exhibit a rapid response (either an increase or a decrease) to changes in agroeconomic and agrotechnological conditions. In addition, it allows the delineation of areas where yields are more stable and change gradually. The shape of the yield trend is determined by the influence of agro-technological and agro-economic factors, which account for fluctuations in rapeseed yield to a significant extent, ranging from 53 to 90% (Zymaroieva et al., 2020). The yield of corn is subject to the influence of spatially determined processes that exhibit oscillatory dynamics with varying periodicity. The analysis of geographically weighted principal components revealed the existence of spatially non-stationary environmental regimes that underpin the oscillatory component of temporal variation in corn yield (Zymaroieva, 2019). The analysis of the spatial and temporal dynamics of corn yields revealed the intricate nature of the underlying processes that determine it. A common feature of temporal changes in corn yields across all administrative regions is the presence of a trend that can be described by a fourth-degree polynomial. The characteristic points of the fourth-degree polynomial curve can be interpreted and used to describe the yield dynamics in a meaningful way.

The regression analysis demonstrates that the overall trend in yield dynamics is determined by a combination of agrotechnological and agroeconomic factors. The coefficient of determination of the regression model can be interpreted as an indicator of the extent to which agrotechnological and agroeconomic factors influence the dynamics of yields. The northern and western districts of the region are the most susceptible to the influence of these factors, whereas the southern districts exhibit the least sensitivity (Zymaroieva, 2019a).

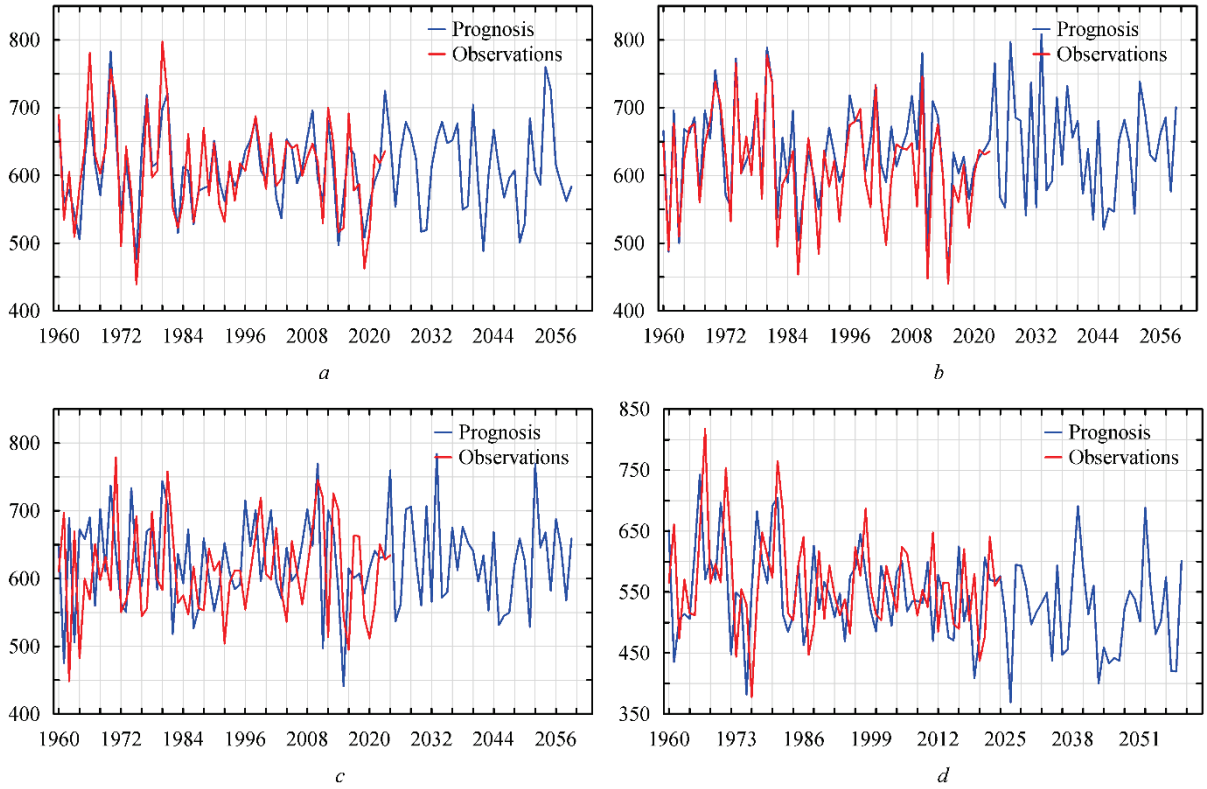

Fig. 4. Observed annual precipitation (mm) and estimated precipitation based on a regression model with temporal AEM variables as predictors for the period 1960–2023 and forecast to 2060: *a* – Nizhyn district, Chernihiv region; *b* – Bilohirsk district, Khmelnytskyi region; *c* – Dubno district, Rivne region; *d* – Kaniv district, Cherkasy region

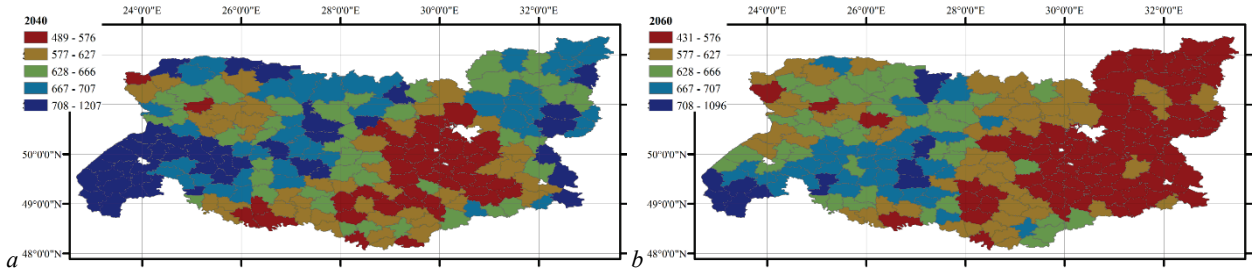

Fig. 5. Spatial variation of annual precipitation (mm) in 2040 (*a*) and 2060 (*b*)

The variability of climate has an impact on corn yields in the Polissia and Forest-Steppe regions of Ukraine. The primary climatic factors that influence crop yields are the continental climate, temperature variability during extreme periods of the year, the degree of temperature variability, and the contrast of temperature conditions (Zymaroieva, 2019a). The dynamics of grain and legume yields are described by an absolute term that reflects the initial conditions of soil fertility in the initial period of research and the indicators of the maximum rate of yield decline in the 1990s and the maximum rate of yield growth in the 2000s. The indicators of the maximum rate of yield decline and the maximum rate of yield growth can be employed as markers of agroecosystem resilience to external factors. The agroecological systems in Ukraine's regions have not yet reached their maximum ecological capacity, and the current limitations are primarily due to agroeconomic and agro-technological factors (Zymaroieva et al., 2019).

The analysis of geographically weighted principal components revealed that soybean yields are influenced by four spatially determined processes that exhibit oscillatory dynamics with varying periodicity. The hypothesis that these oscillatory phenomena are of an environmental nature was validated. The application of geographically weighted principal component analysis has enabled the identification of spatial units exhibiting comparable oscillatory components of soybean yield variation. In Polissia and the Forest-Steppe, specific patterns of time dynamics of soybean yields were identified within homogeneous zones, which exhibited qualitative differences between zones. The patterns of temporal dynamics of soybean yields were found to be uniform within certain territorial areas. Thus, such areas are homogeneous in terms of the influence and dynamics of environmental factors, which provided the basis for interpreting these areas as agroecological zones of soybean cultivation (Zymaroieva et al., 2019). The regression analysis demonstrated that the agrotechnological and agroclimatic regimes of agricultural production are the primary factors influencing the general trend of rye yield dynamics (Kunah et al., 2018). A model was constructed to examine the factors contributing to water erosion in the Volyn region. An increase in precipitation contrast in either space or time can result in heightened erosion processes, reaching a point where the precipitation intensity itself is affected by this contrast. Furthermore, temporal AEM predictors, which are a composite of independent data vectors, are also effective at modelling the patterns of variability over time.

The capacity to be characterised by AEM predictors is more pronounced in the relatively flat regions of the study area. This is consistent with the findings that precipitation in areas with more complex terrain is less

well described by regular patterns and, therefore, can be predicted over time (Dorninger et al., 2008). The temporal modelling of precipitation dynamics over a period of more than 60 years can be accomplished with the assistance of eight AEM predictors, which represent temporal patterns of varying frequencies and amplitudes. If it is assumed that the established oscillatory dynamics will continue into the coming decades, then these AEM predictors can be extended to encompass the desired time period, and a regression model can be employed to obtain a forecast of precipitation dynamics in the near future.

Table 2
Parameters of the asymmetric Gaussian model of precipitation impact on crop yields

Agricultural crop*	Parameter**	Estimate	Std.error	*t*-value	*P*-level
Maize (500–800 mm) L = 1097 mm	Eta	0.05	0.11	0.47	0.64
	Beta	–1.16	0.01	–82.84	< 0.001
	Delta	591.38	4.08	120.50	< 0.001
	Sigma1	11.72	4.18	2.80	0.01
	Sigma2	920.35	0.91	1009.76	< 0.001
Potato (450–700 mm) L = 187 mm	Eta	0.01	0.01	6.10	< 0.001
	Beta	–0.02	0.01	–17.53	< 0.001
	Delta	479.90	1.88	255.91	< 0.001
	Sigma1	0.97	1.60	0.61	< 0.001
	Sigma2	157.90	0.74	214.70	< 0.001
Rapeseed (500–700 mm) L = 2536 mm	Eta	0.07	12.60	0.01	1.00
	Beta	–2.72	0.02	–112.91	< 0.001
	Delta	658.30	40.73	16.16	< 0.001
	Sigma1	309.40	814.00	0.38	0.70
	Sigma2	1760.00	18.93	929.72	< 0.001
Rye (400–1000 mm) L = 1178 mm	Eta	0.16	0.00	0.35	0.73
	Beta	–0.04	0.00	–58.56	< 0.001
	Delta	489.80	5.22	93.82	< 0.001
	Sigma1	9.60	5.11	1.88	0.05
	Sigma2	990.90	1.24	801.23	< 0.001
Soybean (450–700 mm) L = 309 mm	Eta	0.16	0.06	2.79	0.01
	Beta	–0.75	0.02	–45.05	< 0.001
	Delta	502.64	4.72	106.49	< 0.001
	Sigma1	14.90	4.71	3.16	< 0.001
	Sigma2	990.90	1.24	801.23	< 0.001
Sugar beet (550–750 mm) L = 260 mm	Eta	3.35	2.62	1.28	0.20
	Beta	–13.02	0.40	–32.83	< 0.001
	Delta	614.14	6.00	102.29	< 0.001
	Sigma1	142.66	22.47	6.35	< 0.001
	Sigma2	78.14	35.00	2.23	0.03
Sunflower (600–1000 mm) L = 834 mm	Eta	0.02	0.28	0.07	0.94
	Beta	–0.99	0.02	–57.02	< 0.001
	Delta	784.71	61.73	9.47	< 0.001
	Sigma1	249.82	176.05	1.42	0.16
	Sigma2	458.64	46.01	–9.97	< 0.001
Vegetables (600–900 mm) L = 886 mm	Eta	0.01	0.09	0.07	0.94
	Beta	–0.43	0.02	–23.30	< 0.001
	Delta	641.60	13.75	39.38	< 0.001
	Sigma1	26.94	14.87	1.81	0.05
	Sigma2	725.70	3.64	199.62	< 0.001
Wheat (500–800 mm) L = 1091 mm	Eta	0.03	0.08	0.42	0.67
	Beta	–0.12	0.02	–6.64	< 0.001
	Delta	717.18	14.22	50.43	< 0.001
	Sigma1	200.97	94.07	2.14	0.03
	Sigma2	725.70	3.64	199.62	< 0.001

Note: * are the indicative values of crop water needs according to FAO and L is the crop tolerance; ** are the parameters of the asymmetric bell-shaped curve: eta is the maximum value of y, beta is the parameter controlling the lower values, delta is the break-point separating the first and second half-bell curve, sigma1 is the scale for the first half of the bell-shaped curve which is the rate of culture yield increase due to precipitation increase, sigma2 is the scale for the second half of the bell-shaped curve which is the rate of culture yield decrease due to precipitation increase.

The forecast indicates a downward trend in precipitation, particularly in areas with the most developed agriculture. Climate variability exerts a direct or indirect influence on crop production (Guimarães Nobre et al., 2019). The response of the yields of the most important crops in the region to precipitation can be most accurately described by an asymmetric bell-shaped model. The estimates of the optimum derived from this model are in good agreement with the reference data for the respective crops. However, the aforementioned reference data lack information regarding the shape of the response curve to the environmental factor. It is crucial to highlight that for the overwhelming majority of crops, the curve's left-hand side is markedly steeper, indicating a markedly high sensitivity of yields to reduced precipitation. Conversely, crops exhibit a markedly delayed response to increased precipitation. These patterns indicate that the projected decrease in precipitation in the area of active agricultural production carries significant risks of reducing crop yields in the coming decades.

Conclusion

The analysis of precipitation dynamics for the period 1960–2023 indicates that 95.1% of precipitation variability can be described by spatial MEM variables. The RDA approach enables the decomposition of precipitation variability into eight RDA axes, which are distinguished by a particular spatial hierarchical structure resulting from the combination of broad-, medium-, and fine-scale spatial patterns. The occurrence of precipitation at a broad scale is influenced by geographical factors, including the zonation of longitude and latitude. Medium-scale patterns of variability are the result of the influence of geological and morphological factors on precipitation dynamics, which are also reflected in the structure of the soil cover. As a consequence, soil characteristics can be considered reliable predictors of the corresponding climate patterns. The fine-scale patterns can be attributed to the influence of landscape diversity. The zonal pattern exhibited variations as a consequence of anthropogenic factors. The presence of agricultural land has a significant impact on the intensity of moisture evaporation from the Earth's surface, which in turn affects the precipitation regime. The impact of natural landscapes on the water balance of territories is a significant factor in the formation of the spatially hierarchical structure of precipitation. Furthermore, patterns of variability over time can be effectively modelled using temporal AEM predictors, which are a composite of independent data vectors. The forecast indicates a downward trend in precipitation in the coming decades, particularly in areas where agriculture is most developed. The response of yields of the most important crops in the region to precipitation can best be described by an asymmetric bell-shaped model. The vast majority of crops are highly sensitive to reduced precipitation. The projected decline in precipitation in the area of active agricultural production carries significant risks of a decrease in crop yields in the coming decades.

References

Augustine, D. J. (2010). Spatial versus temporal variation in precipitation in a semiarid ecosystem. Landscape Ecology, 25(6), 913–925.

Baho, D. L., Futter, M. N., Johnson, R. K., & Angeler, D. G. (2015). Assessing temporal scales and patterns in time series: Comparing methods based on redundancy analysis. Ecological Complexity, 22, 162–168.

Benziane, S. (2024). Survey: Rainfall prediction precipitation, review of statistical methods. Wseas Transactions on Systems, 23, 47–59.

Blanchet, F. G., Legendre, P., & Borcard, D. (2008). Modelling directional spatial processes in ecological data. Ecological Modelling, 215(4), 325–336.

Blyth, E. M., Evans, J. G., Finch, J. W., Bantges, R., & Harding, R. J. (2006). Spatial variability of the English agricultural landscape and its effect on evaporation. Agricultural and Forest Meteorology, 138(1–4), 19–28.

Bougara, H., Hamed, K. B., Borgemeister, C., Tischbein, B., & Kumar, N. (2020). Analyzing trend and variability of rainfall in the Tafna basin (Northwestern Algeria). Atmosphere, 11(4), 347.

Butler, E. E., & Huybers, P. (2013). Adaptation of US maize to temperature variations. Nature Climate Change, 3(1), 68–72.

Charles, A. C., Armstrong, A., Nnamdi, O. C., Innocent, M. T., Obiageri, N. J., Begianpuye, A. F., & Timothy, E. E. (2024). Review of spatial analysis as a geographic information management tool. American Journal of Engineering and Technology Management, 9(1), 8–20.

Chen, J., Franklin, J. F., & Lowe, J. S. (1996). Comparison of abiotic and structurally defined patch patterns in a hypothetical forest landscape. Conservation Biology, 10(3), 854–862.

Chen, J., Franklin, J. F., & Spies, T. A. (1993). Contrasting microclimates among clearcut, edge, and interior of old-growth Douglas-fir forest. Agricultural and Forest Meteorology, 63(3–4), 219–237.

Claußnitzer, A., & Névir, P. (2009). Analysis of quantitative precipitation forecasts using the Dynamic State Index. Atmospheric Research, 94(4), 694–703.

Dorninger, M., Schneider, S., & Steinacker, R. (2008). On the interpolation of precipitation data over complex terrain. Meteorology and Atmospheric Physics, 101(3–4), 175–189.

Dray, S., Legendre, P., & Peres-Neto, P. R. (2006). Spatial modelling: A comprehensive framework for principal coordinate analysis of neighbour matrices (PCNM). Ecological Modelling, 196(3–4), 483–493.
Ellouze, M., Azri, C., & Abida, H. (2009). Spatial variability of monthly and annual rainfall data over Southern Tunisia. Atmospheric Research, 93(4), 832–839.
Emmanuel, I., Andrieu, H., Leblois, E., & Flahaut, B. (2012). Temporal and spatial variability of rainfall at the urban hydrological scale. Journal of Hydrology, 430–431, 162–172.
Forman, R. (1995). Land mosaics. The ecology of landscapes and regions. Cambridge University Press, Cambridge.
Guimarães Nobre, G., Hunink, J. E., Baruth, B., Aerts, J. C. J. H., & Ward, P. J. (2019). Translating large-scale climate variability into crop production forecast in Europe. Scientific Reports, 9(1), 1277.
Harbar, O., Moroz, V., Harbar, D., Vyskushenko, D., & Kratiuk, O. (2024). Spatial variation of earthworm communities in the motorway proximity. Studia Biologica, 18(2), 157–168.
Hendri, E. P., & Fadhlia, S. (2024). Times series data analysis: The Holt-Winters model for rainfall prediction in West Java. International Journal of Applied Mathematics, Sciences, and Technology for National Defense, 2(1), 1–8.
Hernández-Rodríguez, M., Romo-Lozano, J. L., Barrios-Puente, G., & Cuevas-Alvarado, C. M. (2023). Climate change and its effects on agriculture in Mexico. Agrociencia, 1(1), 1–14.
Hird, J. N., & McDermid, G. J. (2009). Noise reduction of NDVI time series: An empirical comparison of selected techniques. Remote Sensing of Environment, 113(1), 248–258.
Jonsson, P., & Eklundh, L. (2002). Seasonality extraction by function fitting to time-series of satellite sensor data. IEEE Transactions on Geoscience and Remote Sensing, 40(8), 1824–1832.
Kassaye, S. M., Tadesse, T., Tegegne, G., & Tadesse, K. E. (2022). The sensitivity of meteorological dynamics to the variability in catchment characteristics. Water, 14(22), 3776.
Kraan, C., Dormann, C. F., Greenfield, B. L., & Thrush, S. F. (2015). Cross-scale variation in biodiversity-environment links illustrated by coastal sandflat communities. PLoS One, 10(11), e0142411.
Kukol, K., Pukhtaievych, P., Vorobey, N., & Kots, T. (2024). Impact of biological fungicides on the formation and functioning of symbiotic system soybean–*Bradyrhizobium japonicum*. Studia Biologica, 18(2), 97–110.
Kunah, O. M., Pakhomov, O. Y., Zymaroieva, A. A., Demchuk, N. I., Skupskyi, R. M., Bezuhla, L. S., & Vladyka, Y. P. (2018). Agroeconomic and agroecological aspects of spatial variation of rye (*Secale cereale*) yields within Polesia and the Forest-Steppe zone of Ukraine: The usage of geographically weighted principal components analysis. Biosystems Diversity, 26(4), 276–285.
Kunakh, O. M., Volkova, A. M., Tutova, G. F., & Zhukov, O. V. (2023). Diversity of diversity indices: Which diversity measure is better? Biosystems Diversity, 31(2), 131–146.
Kunakh, O. M., Yorkina, N. V., Zhukov, O. V., Turovtseva, N. M., Bredikhina, Y. L., & Logvina-Byk, T. A. (2020). Recreation and terrain effect on the spatial variation of the apparent soil electrical conductivity in an urban park. Biosystems Diversity, 28(1), 3–8.
Kyyak, V., Bilonoha, V., & Kyyak, N. (2023). Spatial and functional structure of the population area in plants – the need for differentiation. Studia Biologica, 17(4), 173–186.
Latif, S. D., Alyaa Binti Hazrin, N., Hoon Koo, C., Lin Ng, J., Chaplot, B., Feng Huang, Y., El-Shafie, A., & Najah Ahmed, A. (2023). Assessing rainfall prediction models: Exploring the advantages of machine learning and remote sensing approaches. Alexandria Engineering Journal, 82, 16–25.
Leng, G., & Hall, J. W. (2020). Predicting spatial and temporal variability in crop yields: An inter-comparison of machine learning, regression and process-based models. Environmental Research Letters, 15(4), 044027.
Lewis-Beck, C., Walker, V. A., Niemi, J., Caragea, P., & Hornbuckle, B. K. (2020). Extracting agronomic information from SMOS vegetation optical depth in the us corn belt using a nonlinear hierarchical model. Remote Sensing, 12(5), 827.
Lobachevska, O., & Karpinets, L. (2024). Water exchange of the forest ecosystems epigeic bryophytes depending on changes of the structural and functional organization of their turfs and the influence of local growth environmental conditions. Studia Biologica, 18(2), 139–156.
Mughal, M. O., Kubilay, A., Fatichi, S., Meili, N., Carmeliet, J., Edwards, P., & Burlando, P. (2021). Detailed investigation of vegetation effects on microclimate by means of computational fluid dynamics (CFD) in a tropical urban environment. Urban Climate, 39, 100939.
Mykhailyuk, T., Lisovets, O., & Tutova, H. (2023). The importance of terrain factors in the spatial variability of plant cover diversity in a steppe gully. Biosystems Diversity, 31(4), 470–483.
Nguyen, T. T., Ngo, H. H., Guo, W., Wang, X. C., Ren, N., Li, G., Ding, J., & Liang, H. (2019). Implementation of a specific urban water management – Sponge City. Science of the Total Environment, 652, 147–162.
Papalaskaris, T., Panagiotidis, T., & Pantrakis, A. (2016). Stochastic monthly rainfall time series analysis, modeling and forecasting in Kavala City, Greece, North-Eastern Mediterranean Basin. Procedia Engineering, 162, 254–263.
Pham, B. T., Le, L. M., Le, T.-T., Bui, K.-T. T., Le, V. M., Ly, H.-B., & Prakash, I. (2020). Development of advanced artificial intelligence models for daily rainfall prediction. Atmospheric Research, 237, 104845.
Qingming, W., Shan, J., Jiaqi, Z., Guohua, H., Yong, Z., Yongnan, Z., Xin, H., Haihong, L., Lizhen, W., Fan, H., & Changhai, Q. (2022). Effects of vegetation restoration on evapotranspiration water consumption in mountainous areas and assessment of its remaining restoration space. Journal of Hydrology, 605, 127259.
Roldán-Valcarce, A., Jato-Espino, D., Manchado, C., Bach, P. M., & Kuller, M. (2023). Vulnerability to urban flooding assessed based on spatial demographic, socio-economic and infrastructure inequalities. International Journal of Disaster Risk Reduction, 95, 103894.
Sang, Y.-F., Fu, Q., Singh, V. P., Sivakumar, B., Zhu, Y., & Li, X. (2020). Does summer precipitation in China exhibit significant periodicities? Journal of Hydrology, 581, 124289.
Sariş, F., Hannah, D. M., & Eastwood, W. J. (2010). Spatial variability of precipitation regimes over Turkey. Hydrological Sciences Journal, 55(2), 234–249.
Sayemuzzaman, M., & Jha, M. K. (2014). Seasonal and annual precipitation time series trend analysis in North Carolina, United States. Atmospheric Research, 137, 183–194.
Seo, S. B., Das Bhowmik, R., Sankarasubramanian, A., Mahinthakumar, G., & Kumar, M. (2019). The role of cross-correlation between precipitation and temperature in basin-scale simulations of hydrologic variables. Journal of Hydrology, 570, 304–314.
Steele, B. M., Reddy, S. K., & Nemani, R. R. (2005). A regression strategy for analyzing environmental data generated by spatio-temporal processes. Ecological Modelling, 181(2–3), 93–108.
Wagner, H. H. (2013). Rethinking the linear regression model for spatial ecological data. Ecology, 94(11), 2381–2391.
Wallis, K. F. (2014). The two-piece normal, binormal, or double gaussian distribution: Its origin and rediscoveries. Statistical Science, 29(1), 106–112.
Wei, J., & Dirmeyer, P. A. (2019). Sensitivity of land precipitation to surface evapotranspiration: A nonlocal perspective based on water vapor transport. Geophysical Research Letters, 46(21), 12588–12597.
Wu, J., & David, J. L. (2002). A spatially explicit hierarchical approach to modeling complex ecological systems: Theory and applications. Ecological Modelling, 153(1–2), 7–26.
Zymaroieva, A. (2019a). Assessment of the climate changes impact on the productivity of maize within the Polissya and Forest Steppe ecoregions within Ukraine. Scientific Horizons, 84(11), 113–120.
Zymaroieva, A. (2019b). Spatio-temporal patterns of maize yield variation within Ukraine. Scientific Horizons, 75(2), 58–66.
Zymaroieva, A. (2019c). The perspectives of the application of geographically weighted principal components analysis for estimation of maize yields spatial variability. Scientific Horizons, 83(10), 20–27.
Zymaroieva, A., & Zhukov, O. (2020). Analyzing cereal and grain legumes (pulses) yields patterns in the forest and forest-steppe zones of Ukraine using geographically weighted principal components analysis. Acta Agriculturae Slovenica, 116(2), 287.
Zymaroieva, A., Pinkina, T., Ivanyuk, T., & Tyshkovskyy, V. (2019). Evaluation of correlation between maize yield parameters and landscape diversity indicators. Scientific Horizons, 86(1), 29–38.
Zymaroieva, A., Zhukov, O., & Romanchuck, L. (2020). The spatial patterns of long-term temporal trends in yields of soybean (*Glycine max* (L.) Merril) in the Central European Mixed Forests (Polissya) and East European Forest Steppe ecoregions within Ukraine. Journal of Central European Agriculture, 21(2), 320–332.
Zymaroieva, A., Zhukov, O., Fedoniuk, T., Pinkina, T., & Hurelia, V. (2021). The relationship between landscape diversity and crops productivity: Landscape scale study. Journal of Landscape Ecology, 14(1), 39–58.
Zymaroieva, A., Zhukov, O., Fedoniuk, T., Pinkina, T., & Vlasiuk, V. (2021). Edaphoclimatic factors determining sunflower yields spatiotemporal dynamics in Northern Ukraine. Oilseeds and Fats, Crops and Lipids, 28, 26.
Zymaroieva, A., Zhukov, O., Fedonyuk, T., & Pinkin, A. (2019). Application of geographically weighted principal components analysis based on soybean yield spatial variation for agro-ecological zoning of the territory. Agronomy Research, 17(6), 2460–2473.
Zymaroieva, A., Zhukov, O., Fedonyuk, T., & Pinkina, T. (2020). The spatio-temporal trend of rapeseed yields in Ukraine as a marker of agro-economic factors influence. Agronomy Research, 18(S2), 1584–1596.
Zymaroieva, A., Zhukov, O., Romanchuck, L., & Pinkin, A. (2019). Spatiotemporal dynamics of cereals grains and grain legumes yield in Ukraine. Bulgarian Journal of Agricultural Science, 25(6), 1107–1113.